International Journal of Chemistry; Vol. 16, No. 1; 2024
ISSN 1916-9698 E-ISSN 1916-9701
Published by Canadian Center of Science and Education

Crystal Growth and Structure of $NiC_4H_4O_6 \cdot 2.5H_2O$

Takanori Fukami[1], Shuta Tahara[1]

[1]Department of Physics and Earth Sciences, Faculty of Science, University of the Ryukyus, Japan

Correspondence: Takanori Fukami, Department of Physics and Earth Sciences, Faculty of Science, University of the Ryukyus, Okinawa 903-0213, Japan. E-mail: fukami@sci.u-ryukyu.ac.jp

Received: September 15, 2023 Accepted: October 27, 2023 Online Published: October 30, 2023

doi:10.5539/ijc.v16n1p1 URL: https://doi.org/10.5539/ijc.v16n1p1

Abstract

Single crystals of nickel tartrate hemi-pentahydrate, $NiC_4H_4O_6 \cdot 2.5H_2O$, were grown by the gel method using silica gels. The crystal structure was determined by the single-crystal X-ray diffraction method. Its structure was orthorhombic with space group $P2_12_12_1$ and lattice constants a = 7.8578(3) Å, b = 11.0988(5) Å, and c = 18.0529(8) Å, and consisted of slightly distorted NiO_6 octahedra, $C_4H_4O_6$ and H_2O molecules, $C_4H_4O_6$–Ni–$C_4H_4O_6$ chains containing H_2O molecules, and O–H···O hydrogen-bonded frameworks between adjacent molecules. The $C_4H_4O_6$ molecules contained both single and double C–O bonds, and single C–C bonds, similar to other tartrate compounds. We discussed the differences in the chemical formulae and structures of tartrate compounds induced by different cations of the first transition metal series.

Keywords: $NiC_4H_4O_6 \cdot 2.5H_2O$, gel method, crystal structure, X-ray diffraction

1. Introduction

Tartrate compounds are formed by the reaction of tartaric acid with compounds containing positive ions (i.e., two monovalent cations or one divalent cation) (Desai & Patel, 1988; Fukami & Tahara, 2020; Fukami & Tahara, 2021; Fukami & Tahara, 2022; Labutina, Marychev, Portnov, Somov, & Chuprunov, 2011). Tartaric acid ($C_4H_6O_6$; systematic name: 2,3-dihydroxybutanedioic acid) has two chiral carbon atoms in its structure, which provides the possibility for four different forms of chiral, racemic, and achiral isomers as follows: L(+)-tartaric, D(–)-tartaric, racemic (DL-) tartaric, and meso-tartaric acid (Bootsma & Schoone, 1967; Fukami, Tahara, Yasuda, & Nakasone, 2016; Song, Teng, Dong, Ma, & Sun, 2006). Some of these compounds are of interest in research because of their physical properties, particularly their excellent dielectric, ferroelectric, piezoelectric, and nonlinear optical properties (Abdel-Kader et al., 1991; Firdous, Quasim, Ahmad, & Kotru, 2010; Torres et al., 2002). Moreover, they were formerly used in various industrial applications, for example, as transducers and optical parts.

Recently, we reported the crystal growth, structure, and thermal properties of $FeC_4H_4O_6 \cdot 2.5H_2O$ (Fukami & Tahara, 2022). The single crystals were grown by the gel method using silica gels. The space group symmetry (orthorhombic $P2_12_12_1$) and structural parameters of the crystal were determined at room temperature. Its structure consisted of slightly distorted FeO_6 octahedra, $C_4H_4O_6$ and H_2O molecules, $C_4H_4O_6$–Fe–$C_4H_4O_6$ chains joined via Fe–O bonds, and O–H···O hydrogen-bonding frameworks between adjacent molecules. Weight losses due to the thermal decomposition of the crystal were observed in the temperature range of 300–1060 K, and were suggested to be caused by the evaporation of bound water molecules and the evolution of H_2CO, CO, and O_2 gases from $C_4H_4O_6$ molecules. The black residue obtained after decomposition was composed of triiron tetraoxide (Fe_3O_4) and carbon. Labutina et al. (Labutina, Marychev, Portnov, Somov, & Chuprunov, 2011) have grown many tartrate single crystals by the gel method, and determined the crystal system and lattice parameters (lattice constants and angles). However, a nickel tartrate compound, which is formed by the reaction of tartaric acid with nickel ions, has not been synthesized yet.

In this study, we report the growth of $NiC_4H_4O_6 \cdot 2.5H_2O$ single crystals by the gel method, and the crystal structure was determined by single-crystal X-ray diffraction method.

2. Experimental

2.1 Crystal Growth

The $NiC_4H_4O_6 \cdot 2.5H_2O$ crystals were grown at room temperature by the gel method using silica gels. The gels were prepared in test tubes (length of 200 mm and diameter of 30 mm) using aqueous solutions of Na_2SiO_3 (20 ml of 1.0 M), $C_4H_6O_6$ (20 ml of 1.0 M), and CH_3COOH (25 ml of 3.0 M), and aged for seven days. Thereafter, a solution of $Ni(NO_3)_2 \cdot 6H_2O$ (20 ml of 0.5 M) was gently poured on top of the gel. The crystals were harvested after approximately

20 months. The following reaction is expected to occur during the growth process:

$$2Ni(NO_3)_2{\cdot}6H_2O + 2C_4H_6O_6 \rightarrow 2(NiC_4H_4O_6{\cdot}2.5H_2O) + 4HNO_3 + 7H_2O.$$

Figure 1 shows the photograph of single crystals and polycrystalline aggregates of $NiC_4H_4O_6{\cdot}2.5H_2O$. Single crystals and polycrystalline aggregates were grown in the gel medium. The polycrystalline aggregates, which were quasi-spherical in shape and green in color, were very similar to those of $FeC_4H_4O_6{\cdot}2.5H_2O$ aggregates reported in the previous papers, except for the difference in color (Dhikale, Shitole, Nahire, & Chavan, 2019; Fukami & Tahara, 2022; Mathivanan & Haris, 2013).

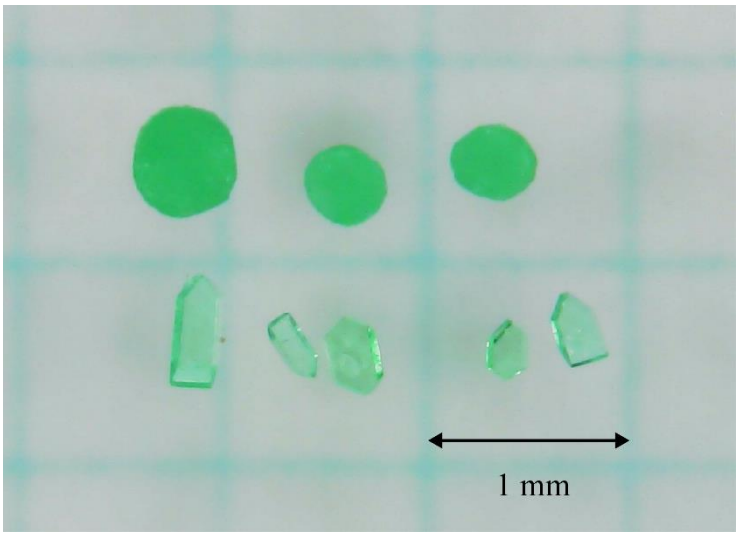

Figure 1. Photograph of single and polycrystalline $NiC_4H_4O_6{\cdot}2.5H_2O$ crystals

2.2 X-ray Measurements

The X-ray diffraction measurements were performed using a Rigaku Saturn CCD X-ray diffractometer with graphite-monochromated Mo K_α radiation (λ = 0.71073 Å). Single-crystal diffraction data for the $NiC_4H_4O_6{\cdot}2.5H_2O$ crystal were collected at 299 K using an ω scan mode with a crystal-to-detector distance of 40 mm, and processed using the CrystalClear software package. The intensity data were corrected for Lorentz polarization and absorption effects. The crystal structure was solved by direct methods using the SIR2014 program and refined on F^2 by full-matrix least-squares methods using the SHELXL-2017 program in the WinGX package (Burla et al., 2015; Farrugia, 2012; Sheldrick, 2015).

3. Results and Discussion

3.1 Structure Determination

The crystal structure of $NiC_4H_4O_6{\cdot}2.5H_2O$ was determined at room temperature. The lattice parameters calculated from all observed X-ray reflections showed that the crystal belongs to the orthorhombic system, and the systematic extinctions indicated that the space group is $P2_12_12_1$. The obtained lattice parameters were similar to those of $FeC_4H_4O_6{\cdot}2.5H_2O$ (Fukami & Tahara; 2022). All non-hydrogen atoms were refined anisotropically, and hydrogen atoms located on difference electron density maps were refined isotropically. Positional and thermal parameters for ten hydrogen atoms of water molecules, which did not converge to reasonable values, were fixed during the refinement. A final R-factor of 3.54% was calculated for 6245 unique observed reflections.

The relevant crystal data, and a summary of the intensity data collection and structure refinement are shown in Table 1. Figure 2 shows the projection along the a-axis of the $NiC_4H_4O_6{\cdot}2.5H_2O$ structure. The positional parameters in fractions of the unit cell and the thermal parameters are listed in Table 2. Selected bond lengths and angles are shown in Table 3, and hydrogen-bond geometries are presented in Table 4.

Table 1. Crystal data, intensity data collections, and structure refinements for $NiC_4H_4O_6{\cdot}2.5H_2O$

Compound, M_r	$Ni_2O_{17}C_8H_{18}$, 503.64
Measurement temperature	299 K
Crystal system, space group	Orthorhombic, $P2_12_12_1$
Lattice constants	a = 7.8578(3) Å, b = 11.0988(5) Å
	c = 18.0529(8) Å
V, Z	1574.4(1) Å^3, 4
D(cal.), μ(Mo K_α), F(000)	2.125 Mg·m^{-3}, 2.489 mm^{-1}, 1032
Crystal size	0.20×0.20×0.10 mm^3
θ range for data collection	2.15–33.99°
Index ranges	$-12 \le h \le 12$, $-17 \le k \le 17$, $-28 \le l \le 28$
Reflections collected, unique	29265, 6428 [R(int) = 0.0381]
Completeness to θ_{max}	100%
Absorption correction type	Numerical
Transmission factor T_{min}–T_{max}	0.6015–0.8134
Date, parameter	6245 [$I > 2\sigma(I)$], 277
Final R indices	R_1 = 0.0354, wR_2 = 0.0727
R indices (all data)	R_1 = 0.0369, wR_2 = 0.0737
Weighting scheme	$w = 1/[\sigma^2(F_o^2)+(0.029P)^2+0.687P]$
	$P = (F_o^2+2F_c^2)/3$
Flack parameter	-0.012(5)
Goodness-of-fit on F^2	1.073
Extinction coefficient	0.0005(4)
Largest diff. peak and hole	0.494 / -0.627 eÅ^{-3}

3.2 Structural Elucidation

The crystal structure of $NiC_4H_4O_6{\cdot}2.5H_2O$ comprises two non-equivalent Ni atoms, two crystallographically independent $C_4H_4O_6$ molecules, and five independent H_2O molecules. This structure is identical to that of the $FeC_4H_4O_6{\cdot}2.5H_2O$ crystal (Fukami & Tahara; 2022). Figure 2 shows that the $C_4H_4O_6$ molecules are arranged periodically along the c-axis, and the Ni atoms are located between the $C_4H_4O_6$ molecules. Furthermore, the Ni atoms are bonded to six nearest-neighboring O atoms, forming slightly distorted NiO_6 octahedra, as listed in Table 3. The six O atoms include five O atoms from three $C_4H_4O_6$ molecules and one O atom from the H_2O molecule. Therefore, the three $C_4H_4O_6$ and one H_2O molecules are connected via the Ni–O bonds. The lengths of the Ni–O bonds are in the range of 2.010(2)–2.099(2) Å, and the average Ni–O distance is 2.046 Å. As shown in Table 4 and Fig. 2, the $C_4H_4O_6$ and H_2O molecules are connected by O–H···O hydrogen bonds, and zigzag hydrogen-bonded chains are formed in the ab-planes (in the (1/4)c- and (3/4)c-planes). There are no hydrogen-bonded chains along the c-axis. However, $C_4H_4O_6$–Ni–$C_4H_4O_6$ chains containing H_2O molecules linked via the Ni–O bonds run along the c-axis.

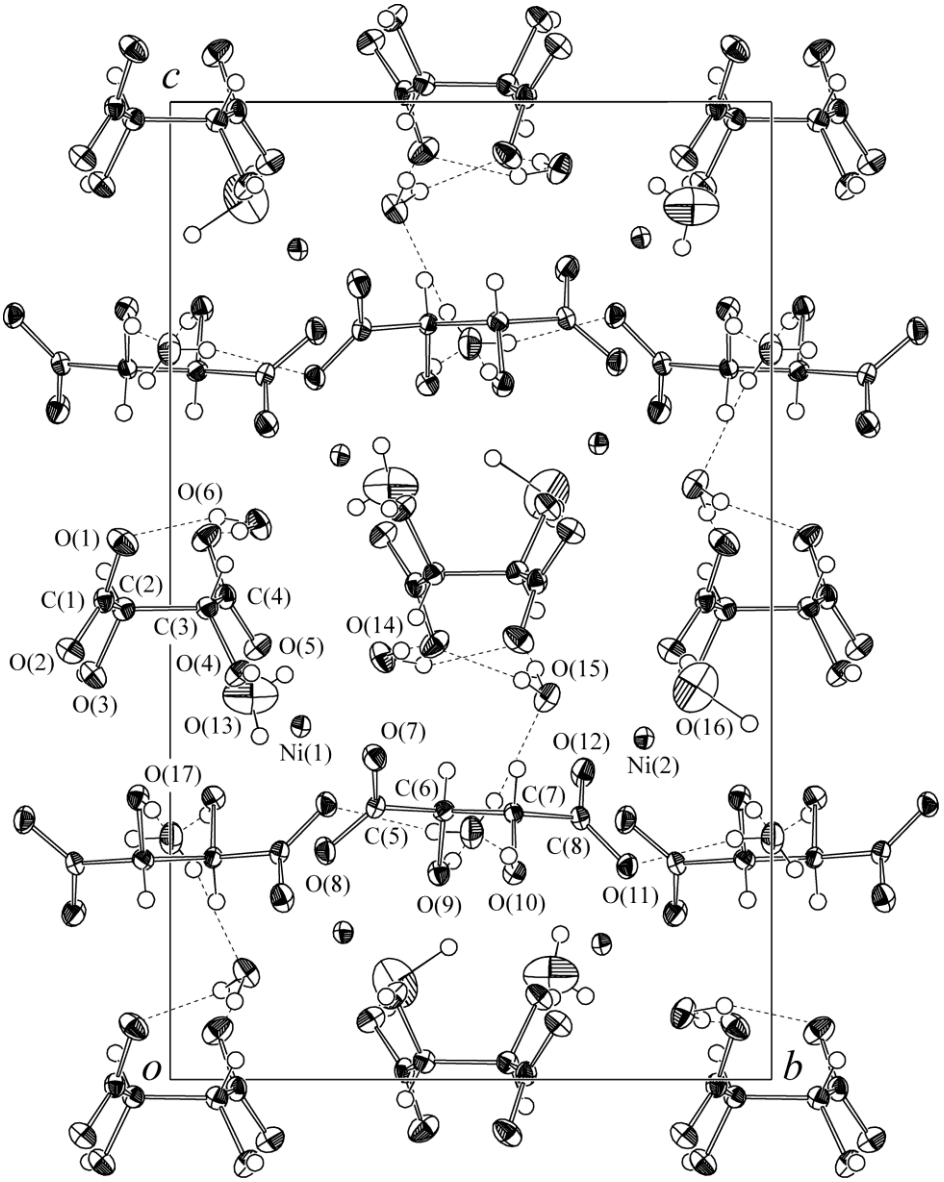

Figure 2. ORTEP projection of the $NiC_4H_4O_6{\cdot}2.5H_2O$ structure along the *a*-axis, with 50% probability-displacement thermal ellipsoids. The solid and dashed short lines indicate O–H···O hydrogen bonds listed in Table 4.

The lengths of six C–O and three C–C bonds in the $C_4H_4O_6$ molecules of $NiC_4H_4O_6{\cdot}2.5H_2O$ are similar to those of other tartrate crystals mentioned in our previous studies (Fukami & Tahara, 2020, 2021, 2022). The comparison of these bond lengths in Table 3 shows that the two C–O bonds of hydroxyl groups in the range of 1.411(3)–1.437(3) Å have a single-bond character, the remaining four bonds in the range of 1.240(3)–1.268(4) Å have a double-bond character, and all the C–C bonds (the range of 1.524(4)–1.545(4) Å) have a single-bond character. The angles between the two least-squares planes of atoms, [C(1)C(2)O(1)O(2)O(3) and C(3)C(4)O(4)O(5)O(6)], and [C(5)C(6)O(7)O(8)O(9) and C(7)C(8)O(10)O(11)O(12)], in the $C_4H_4O_6$ molecules were calculated to be 50.65(9)° and 75.92(8)°, respectively. These angles are similar to those (49.90(8)° and 72.15(7)°) of $FeC_4H_4O_6{\cdot}2.5H_2O$, as reported in the previous study (Fukami & Tahara, 2022).

Table 2. Atomic coordinates and thermal parameters ($\times 10^4$ Å^2) for $NiC_4H_4O_6 \cdot 2.5H_2O$ at room temperature, with standard deviations in parentheses. The anisotropic thermal parameters are defined as $\exp[-2\pi^2(U_{11}a^{*2}h^2+U_{22}b^{*2}k^2+U_{33}c^{*2}l^2+2U_{23}b^*c^*kl+2U_{13}a^*c^*hl+2U_{12}a^*b^*hk)]$. The isotropic thermal parameters (Å^2) for H atoms are listed under U_{11}

Atom	*x*	*y*	*z*	U_{11}	U_{22}	U_{33}	U_{23}	U_{13}	U_{12}
Ni(1)	0.10683(4)	0.21730(3)	0.36139(2)	159(2)	138(1)	171(2)	8(1)	3(1)	5(1)
Ni(2)	0.37453(4)	0.78778(3)	0.34933(2)	164(2)	142(1)	174(2)	1(1)	-3(1)	8(1)
C(1)	0.4395(4)	-0.1102(2)	0.4905(2)	160(12)	144(11)	219(12)	1(9)	-33(9)	31(9)
C(2)	0.2524(4)	-0.0774(3)	0.4813(2)	140(11)	178(11)	196(12)	3(9)	-19(9)	27(9)
C(3)	0.2310(4)	0.0610(3)	0.4824(2)	160(12)	167(11)	177(12)	5(9)	7(9)	22(9)
C(4)	0.0434(4)	0.0919(2)	0.4941(2)	167(12)	155(11)	213(13)	-2(10)	28(10)	3(9)
C(5)	0.8173(4)	0.3418(2)	0.2789(2)	183(12)	128(10)	185(11)	27(9)	-1(9)	5(9)
C(6)	0.7054(4)	0.4550(2)	0.2749(2)	166(12)	165(11)	152(11)	11(9)	2(9)	11(9)
C(7)	0.8112(3)	0.5709(2)	0.2727(2)	160(11)	125(10)	154(11)	-11(8)	3(9)	-3(9)
C(8)	0.6937(4)	0.6817(2)	0.2676(2)	163(12)	132(10)	193(11)	-21(9)	12(9)	-8(8)
O(1)	0.5065(3)	-0.0790(2)	0.5500(1)	250(11)	337(12)	272(11)	-89(10)	-99(9)	77(10)
O(2)	0.5140(3)	-0.1662(2)	0.4386(1)	156(9)	283(11)	237(10)	-55(9)	-29(8)	56(8)
O(3)	0.1921(3)	-0.1278(2)	0.4140(1)	146(9)	241(10)	263(10)	-81(8)	-42(8)	29(8)
O(4)	0.2876(3)	0.1136(2)	0.4156(1)	153(9)	250(10)	240(10)	79(8)	49(7)	33(8)
O(5)	-0.0365(3)	0.1455(2)	0.4427(1)	151(9)	261(10)	241(10)	68(9)	20(8)	27(8)
O(6)	-0.0193(3)	0.0604(2)	0.5544(1)	241(11)	297(11)	265(11)	96(9)	88(9)	60(9)
O(7)	0.9253(3)	0.3398(2)	0.3295(1)	293(12)	202(9)	256(10)	-29(8)	-102(8)	70(8)
O(8)	0.7893(3)	0.2575(2)	0.2342(1)	305(12)	151(9)	276(11)	-25(8)	-93(9)	46(8)
O(9)	0.5958(3)	0.4467(2)	0.2113(1)	190(10)	169(8)	231(9)	-8(7)	-50(8)	16(8)
O(10)	0.9282(3)	0.5723(2)	0.2117(1)	155(9)	190(9)	208(9)	15(7)	29(7)	18(7)
O(11)	0.7238(3)	0.7597(2)	0.2184(1)	266(11)	155(8)	226(10)	16(7)	64(8)	46(7)
O(12)	0.5776(3)	0.6862(2)	0.3141(1)	250(11)	196(9)	305(11)	28(8)	121(9)	58(8)
O(13)	0.6209(4)	0.1334(4)	0.3934(2)	280(15)	1081(30)	512(18)	9(20)	40(15)	-151(18)
O(14)	0.1678(3)	0.3529(2)	0.4320(1)	231(11)	221(10)	346(12)	-77(9)	-54(9)	-8(9)
O(15)	0.3014(3)	0.6266(2)	0.3908(1)	160(9)	243(10)	302(11)	81(9)	52(9)	31(8)
O(16)	0.8574(4)	0.8739(3)	0.4012(2)	194(13)	714(23)	880(25)	169(21)	-40(16)	-58(14)
O(17)	0.7393(3)	0.0015(2)	0.2471(2)	365(14)	187(10)	379(14)	6(9)	7(11)	27(10)
H(1)	0.198(5)	-0.109(3)	0.520(2)	0.02(1)					
H(2)	0.282(4)	0.091(3)	0.527(2)	0.012(8)					
H(3)	0.639(5)	0.460(3)	0.316(2)	0.018(9)					
H(4)	0.872(5)	0.577(3)	0.318(2)	0.017(8)					
H(5)	0.061(6)	-0.141(4)	0.415(3)	0.05(1)					
H(6)	0.399(7)	0.135(4)	0.416(3)	0.05(1)					
H(7)	0.510(9)	0.470(6)	0.224(3)	0.09(2)					
H(8)	1.025(8)	0.563(5)	0.229(3)	0.07(2)					
H(9)	0.663	0.149	0.351	0.06					
H(10)	0.611	0.191	0.414	0.06					
H(11)	0.266	0.384	0.439	0.06					
H(12)	0.111	0.422	0.424	0.06					
H(13)	0.383	0.585	0.409	0.06					
H(14)	0.204	0.607	0.420	0.06					
H(15)	0.758	0.861	0.426	0.06					
H(16)	0.861	0.963	0.364	0.06					
H(17)	0.754	-0.061	0.246	0.06					
H(18)	0.733	0.039	0.215	0.06					

Table 3. Selected interatomic distances (Å^2) and angles (degrees) of $NiC_4H_4O_6 \cdot 2.5H_2O$

Ni(1)–O(4)	2.074(2)	Ni(1)–O(5)	2.014(2)
Ni(1)–O(7)$^{(1)}$	2.053(2)	Ni(1)–O(10)$^{(2)}$	2.099(2)
Ni(1)–O(11)$^{(2)}$	2.017(2)	Ni(1)–O(14)	2.030(2)
Ni(2)–O(2)$^{(3)}$	2.015(2)	Ni(2)–O(3)$^{(3)}$	2.073(2)
Ni(2)–O(8)$^{(4)}$	2.010(2)	Ni(2)–O(9)$^{(4)}$	2.089(2)
Ni(2)–O(12)	2.055(2)	Ni(2)–O(15)	2.023(2)
C(1)–O(1)	1.244(4)	C(1)–O(2)	1.268(3)
C(2)–O(3)	1.420(3)	C(3)–O(4)	1.411(3)
C(4)–O(5)	1.268(4)	C(4)–O(6)	1.245(3)
C(5)–O(7)	1.247(3)	C(5)–O(8)	1.255(3)
C(6)–O(9)	1.437(3)	C(7)–O(10)	1.435(3)
C(8)–O(11)	1.263(3)	C(8)–O(12)	1.240(3)
C(1)–C(2)	1.524(4)	C(2)–C(3)	1.545(4)
C(3)–C(4)	1.528(4)	C(5)–C(6)	1.535(4)
C(6)–C(7)	1.533(4)	C(7)–C(8)	1.541(4)
O(1)–C(1)–O(2)	125.3(3)	O(1)–C(1)–C(2)	115.8(3)
O(2)–C(1)–C(2)	118.9(2)	O(3)–C(2)–C(1)	108.7(2)
O(3)–C(2)–C(3)	111.5(2)	O(4)–C(3)–C(2)	111.5(2)
O(4)–C(3)–C(4)	109.2(2)	O(5)–C(4)–O(6)	125.1(3)
O(5)–C(4)–C(3)	118.8(2)	O(6)–C(4)–C(3)	116.1(3)
O(7)–C(5)–O(8)	125.3(2)	O(7)–C(5)–C(6)	116.0(2)
O(8)–C(5)–C(6)	118.6(2)	O(9)–C(6)–C(5)	109.2(2)
O(9)–C(6)–C(7)	111.1(2)	O(10)–C(7)–C(6)	112.1(2)
O(10)–C(7)–C(8)	109.2(2)	O(11)–C(8)–O(12)	125.9(3)
O(11)–C(8)–C(7)	118.5(2)	O(12)–C(8)–C(7)	115.6(2)
C(1)–C(2)–C(3)	109.9(2)	C(2)–C(3)–C(4)	109.2(2)
C(5)–C(6)–C(7)	112.2(2)	C(6)–C(7)–C(8)	110.3(2)

Symmetry codes: (1) *x*–1,*y*,*z*; (2) –*x*+1,*y*–1/2,–*z*+1/2; (3) *x*,*y*+1,*z*; (4) –*x*+1,*y*+1/2,–*z*+1/2.

Table 4. Hydrogen-bond distances (Å^2) and angles (degrees) of $NiC_4H_4O_6{\cdot}2.5H_2O$

D–H···A	D–H	H···A	D···A	<D–H···A
C(2)–H(1)···O(2)$^{(1)}$	0.90(4)	2.98(4)	3.701(4)	139(3)
C(3)–H(2)···O(7)$^{(2)}$	0.96(3)	2.93(3)	3.882(4)	174(3)
C(6)–H(3)···O(6)$^{(3)}$	0.91(4)	2.66(4)	3.557(4)	169(3)
C(7)–H(4)···O(1)$^{(3)}$	0.95(3)	2.61(3)	3.551(4)	173(3)
O(3)–H(5)···O(16)$^{(4)}$	1.04(5)	1.63(5)	2.640(3)	163(4)
O(4)–H(6)···O(13)	0.91(5)	1.79(5)	2.658(4)	159(5)
O(9)–H(7)···O(17)$^{(5)}$	0.76(7)	2.05(7)	2.804(4)	169(7)
O(10)–H(8)···O(17)$^{(6)}$	0.83(6)	2.02(6)	2.828(3)	165(6)
O(13)–H(9)···O(8)	0.846(3)	2.629(2)	3.451(4)	164.3(3)
O(13)–H(9)···O(17)		2.563(3)	3.159(4)	128.4(3)
O(13)–H(10)···O(6)$^{(3)}$	0.744(4)	3.001(3)	3.696(5)	156.7(3)
O(14)–H(11)···O(6)$^{(3)}$	0.852(2)	1.803(2)	2.651(3)	173.8(2)
O(14)–H(12)···O(1)$^{(2)}$	0.894(2)	1.986(3)	2.831(3)	157.1(2)
O(15)–H(13)···O(6)$^{(3)}$	0.856(2)	1.904(2)	2.696(3)	153.4(2)
O(15)–H(14)···O(1)$^{(2)}$	0.950(2)	1.676(2)	2.606(3)	165.3(2)
O(16)–H(15)···O(2)$^{(7)}$	0.915(3)	1.954(2)	2.817(4)	156.7(2)
O(16)–H(16)···O(10)$^{(6)}$	1.194(4)	2.471(2)	3.442(4)	137.0(2)
O(16)–H(16)···O(17)$^{(7)}$		2.359(3)	3.256(4)	129.9(2)
O(17)–H(17)···O(11)$^{(8)}$	0.706(2)	2.064(2)	2.735(3)	159.1(2)
O(17)–H(18)···O(15)$^{(9)}$	0.712(3)	2.164(2)	2.869(4)	170.6(2)

Symmetry codes: (1) *x*–1/2,–*y*–1/2,–*z*+1; (2) *x*–1/2,–*y*+1/2,–*z*+1; (3) *x*+1/2,–*y*+1/2,–*z*+1; (4) *x*–1,*y*–1,*z*; (5) –*x*+1,*y*+1/2, –*z*+1/2; (6) –*x*+2,*y*+1/2,–*z*+1/2; (7) *x*,*y*+1,*z*; (8) *x*,*y*–1,*z*; (9) –*x*+1,*y*–1/2,–*z*+1/2.

3.3 Cation Effects on the Structure

As mentioned above, we established the crystal structure of the Ni tartrate compound. All structures of tartrate compounds, consisting of divalent cations (from Mn of group 7 to Zn of group 12) belonging to the first transition series, have been elucidated by single crystal X-ray diffraction. Table 5 shows the chemical formulae, space groups, and lattice constants with atomic, ionic, and covalent radii of the cations in the tartrate compounds from articles (Clementi & Raimondi, 1963; Fukami & Tahara, 2020, 2021, 2022; Labutina, Marychev, Portnov, Somov, & Chuprunov, 2011; Slater, 1964, 1965) and Winter's website (Winter, M. J.).

Table 5. Atomic number, chemical symbol, and atomic, ionic, and covalent radii in the first transition series, and chemical formula, space group, and lattice constants of tartrate compounds (Clementi & Raimondi, 1963; Fukami & Tahara, 2020, 2021, 2022; Labutina, Marychev, Portnov, Somov, & Chuprunov, 2011; Slater, 1964, 1965; Winter, M. J.)

Z	Atom	Atomic radius	Ionic radius	Covalent radius	Chemical formula	Space group	*a* (Å)	*b* (Å)	*c* (Å)	*β* (°)
25	Mn	1.61	1.40	1.39	$MnC_4H_4O_6{\cdot}2H_2O$	$P2_1$	7.5901(2)	11.1883(2)	9.0076(3)	99.506(2)
26	Fe	1.56	1.40	1.25	$FeC_4H_4O_6{\cdot}2.5H_2O$	$P2_12_12_1$	7.8905(3)	11.3004(3)	18.3888(6)	
27	Co	1.52	1.35	1.26	$CoC_4H_4O_6{\cdot}2.5H_2O$	$P2_12_12_1$	7.8958(1)	11.1865(2)	18.1876(3)	
28	Ni	1.49	1.35	1.21	$NiC_4H_4O_6{\cdot}2.5H_2O$	$P2_12_12_1$	7.8578(3)	11.0988(5)	18.0529(8)	
29	Cu	1.45	1.35	1.38	$CuC_4H_4O_6{\cdot}3H_2O$	$P2_1$	8.3708(2)	8.7602(1)	12.1373(3)	104.538(1)
30	Zn	1.42	1.35	1.31	$ZnC_4H_4O_6{\cdot}2.5H_2O$	$P2_12_12_1$	7.9292(2)	11.2194(2)	17.9622(4)	

As shown in Table 5, the Mn- and Cu-tartrate compounds contain two and three water molecules in their chemical formulae, respectively. These crystals have monoclinic $P2_1$ symmetry; however, their lattice constants are not close to each other. On the other hand, other crystals consisting of the cations Fe, Co, Ni, or Zn contain 2.5 water molecules in their chemical formulae. They have the same orthorhombic ($P2_12_12_1$) symmetry and nearly identical lattice constants. Thus, the differences in the chemical formulae and structures (space group and lattice constants) are due to the difference of the cation in the compounds. The atomic, ionic, and covalent radii for the Mn atom are 1.61, 1.40, and 1.39 Å, respectively, and for the Cu atoms are 1.45, 1.35, and 1.38 Å, respectively. The radii of the Fe, Co, Ni, and Zn atoms are in the ranges of 1.42–1.56, 1.35–1.40, and 1.21–1.31 Å, respectively. The atomic and ionic radii of the Mn and Cu atoms are close to or in the ranges. However, the covalent radii (1.39 Å of Mn and 1.38 Å of Cu) are out of the range of 1.21–1.31 Å, and larger by approximately 0.1 Å than the average value (1.26 Å) of the range. Thus, it is presumed that the differences in the chemical formulae and structures of the tartrate compounds are correlated with the difference in the covalent radii of the cations.

Tartrate compounds have two independent distorted MO_6 octahedra (M = Mn, Fe, Ni, or Cu) in the unit cell (Fukami & Tahara, 2020; 2021; 2022). Table 6 shows the variation in the range and the average values of twelve M–O bond lengths in the octahedra. There is no remarkable difference between the average values of the bond lengths. However, the longest Mn–O and Cu–O bonds are 2.334(3) and 2.437(2) Å, respectively, and are longer than the longest Fe–O (2.188(2) Å) and Ni–O (2.099(2) Å) bond lengths. The bond length becomes shorter when the bonding strength between two atoms increases. Thus, the bonding strength of the Mn–O and Cu–O bonds is weaker than that of the Fe–O and Ni–O bonds. This is consistent with the fact that the covalent radii of the Mn and Cu atoms are larger than those of the Fe and Ni atoms. Therefore, it is expected that the chemical formulae and structures of the tartrate compounds are highly affected by the bonding strength of the M–O bonds.

Table 6. Variation in the range and average values of twelve M–O bond lengths in the slightly distorted MO_6 octahedra (M = Mn, Fe, Ni, or Cu) of the tartrate compounds previously reported (Fukami & Tahara, 2020; 2021; 2022)

Bond	Range of bond lengths (Å)	Average value (Å)
Mn–O	2.105(2) – 2.334(3)	2.182
Fe–O	2.060(2) – 2.188(2)	2.117
Ni–O	2.010(2) – 2.099(2)	2.046
Cu–O	1.920(1) – 2.437(2)	2.107

4. Summary

Single crystals of nickel tartrate hemi-pentahydrate, $NiC_4H_4O_6{\cdot}2.5H_2O$, were grown at room temperature by the gel method using silica gels. The crystal structure was determined at room temperature by the single-crystal X-ray diffraction technique. The structure was orthorhombic with space group $P2_12_12_1$, and consisted of slightly distorted NiO_6 octahedra, $C_4H_4O_6$ and H_2O molecules, $C_4H_4O_6$–Ni–$C_4H_4O_6$ chains containing H_2O molecules running along the *c*-axis linked via Ni–O bonds, and O–H···O hydrogen-bonded frameworks between adjacent molecules in the *ab*-plane. We studied the differences in the chemical formulae and structures (space group and lattice constants) between tartrate compounds consisting of cations in the first transition series.

Acknowledgments

Not applicable

Authors contributions

Not applicable

Funding

Not applicable

Competing interests

Not applicable

Informed consent

Obtained.

Ethics approval

The Publication Ethics Committee of the Canadian Center of Science and Education.

The journal's policies adhere to the Core Practices established by the Committee on Publication Ethics (COPE).

Provenance and peer review

Not commissioned; externally double-blind peer reviewed.

Data availability statement

The data that support the findings of this study are available on request from the corresponding author. The data are not publicly available due to privacy or ethical restrictions.

Data sharing statement

No additional data are available.

Open access

This is an open-access article distributed under the terms and conditions of the Creative Commons Attribution license (http://creativecommons.org/licenses/by/4.0/).

Copyrights

Copyright for this article is retained by the author(s), with first publication rights granted to the journal.

References

Abdel-Kader, M. M., El-Kabbany, F., Taha, S., Abosehly, A. M., Tahoon, K. K., & El-Sharkawy, A. A. (1991). Thermal and electrical properties of ammonium tartrate. *J. Phys. Chem. Solids*, *52*(5), 655-658. https://doi.org/10.1016/0022-3697(91)90163-T

Bootsma, G. A., & Schoone, J. C. (1967). Crystal structures of mesotartaric acid. *Acta Crystallogr.*, *22*(4), 522-532. https://doi.org/10.1107/S0365110X67001070

Burla, M. C., Caliandro, R., Carrozzini, B., Cascarano, G. L., Cuocci, C., Giacovazzo, C., … & Polidori, G. (2015). Crystal structure determination and refinement via SIR2014. *J. Appl. Crystallogr.*, *48*(1), 306-309. https://doi.org/10.1107/S1600576715001132

Clementi, E., & Raimondi, D. L. (1963). Atomic screening constants from SCF functions. *J. Chem. Phys*., *38*, 2686-2689. https://doi.org/10.1063/1.1733573

Desai, C. C., & Patel, A. H. (1988). Crystal data for ferroelectric $RbHC_4H_4O_6$ and $NH_4HC_4H_4O_6$ crystals. *J. Mater. Sci. Lett.*, *7*(4), 371-373. https://doi.org/10.1007/BF01730747

Dhikale, M. D., Shitole, S. J., Nahire, S. B., & Chavan, A. R. (2019). Electric conductivity study of silica gel grown pure and Cu doped Fe tartrate crystals. *J. Gujarat Res. Society*, *21*(14), 1574-1581. http://www.gujaratresearchsociety.in/index.php/JGRS/article/view/2286

Farrugia, L. J. (2012). WinGX and ORTEP for Windows: an update. *J. Appl. Crystallogr.*, *45*(4), 849-854. https://doi.org/10.1107/S0021889812029111

Firdous, A., Quasim, I., Ahmad, M. M., & Kotru, P. N. (2010). Dielectric and thermal studies on gel grown strontium tartrate pentahydrate crystals. *Bull. Mater. Sci.*, *33*(4), 377-382. https://doi.org/10.1007/s12034-010-0057-1

Fukami, T., & Tahara, S. (2020). Crystal structures and thermal properties of L-$MnC_4H_4O_6{\cdot}2H_2O$ and DL-$MnC_4H_4O_6{\cdot}2H_2O$. *Inter. J. Chem.*, *12*(1), 78-88. https://doi.org/10.5539/ijc.v12n1p78

Fukami, T., & Tahara, S. (2021). Structural and thermal investigations of L-$CuC_4H_4O_6{\cdot}3H_2O$ and DL-$CuC_4H_4O_6{\cdot}2H_2O$ single crystals. *Inter. J. Chem.*, *13*(1), 38-49. https://doi.org/10.5539/ijc.v13n1p38

Fukami, T., & Tahara, S. (2022). Crystal growth, structural and thermal studies of $FeC_4H_4O_6{\cdot}2.5H_2O$, *Inter. J. Chem.*, *14*(2), 8-17. https://doi.org/10.5539/ijc.v14n2p8

Fukami, T., Tahara, S., Yasuda, C., & Nakasone, K. (2016). Structural refinements and thermal properties of L(+)-tartaric, D(-)-tartaric, and monohydrate racemic tartaric acid. *Inter. J. Chem.*, *8*(2), 9-21. https://doi.org/10.5539/ijc.v8n2p9

Labutina, M. L., Marychev, M. O., Portnov, V. N., Somov, N. V., & Chuprunov, E. V. (2011). Second-order nonlinear susceptibilities of the crystals of some metal tartrates. *Crystallogr. Rep.*, *56*(1), 72-74. https://doi.org/10.1134/S1063774510061082

Mathivanan, V., & Haris, M. (2013). Characterization of pure and copper-doped iron tartrate crystals grown in silica gel. *Pramana*, *81*(1), 177-187. https://doi.org/10.1007/s12043-013-0564-x

Sheldrick, G. M. (2015). Crystal structure refinement with SHELXL. *Acta Crystallogr.*, *C71*(1), 3-8. https://doi.org/10.1107/S2053229614024218

Slater, J. C. (1965). Quantum theory of molecules and solids: Symmetry and bonds in crystals. Vol 2. McGraw-Hill, New York

Slater, J. C. (1964). Atomic radii in crystals. *J. Chem. Phys*., *41*, 3199-3204. https://doi.org/10.1063/1.1725697

Song, Q. B., Teng, M. Y., Dong, Y., Ma, C. A., & Sun, J. (2006). (2S,3S)-2,3-Dihydroxy-succinic acid monohydrate. *Acta Crystallogr.*, *E62*(8), o3378-o3379. https://doi.org/10.1107/S1600536806021738

Torres, M. E., Peraza, J., Yanes, A. C., López, T., Stockel, J., López, D. M., Solans, X., Bocanegra, E., & Silgo, C. G. (2002). Electrical conductivity of doped and undoped calcium tartrate. *J. Phys. Chem. Solids*, *63*(4), 695-698. https://doi.org/10.1016/S0022-3697(01)00216-5

Winter, M. J., The periodic table of the elements, all data were quoted from https://www.webelements.com/